Geophysical Research Letters

RESEARCH LETTER
10.1029/2025GL115440

Radial Force Balance in Earth's Magnetotail Thin Current Sheets: MMS Observations

Zhibo Zhang[1], San Lu[1,2,3], Quanming Lu[1,2,3], Rongsheng Wang[1,2,3], Xinmin Li[1], Shimou Wang[1,2,3], and Anton V. Artemyev[4]

[1]School of Earth and Space Sciences, CAS Center for Excellence in Comparative Planetology, CAS Key Laboratory of Geoscience Environment, University of Science and Technology of China, Hefei, China, [2]Deep Space Exploration Laboratory, Hefei, China, [3]Collaborative Innovation Center of Astronautical Science and Technology, Harbin, China, [4]Department of Earth, Planetary, and Space Sciences and Institute of Geophysics and Planetary Physics, University of California, Los Angeles, CA, USA

Key Points:

- We study the radial force balance in magnetotail Thin current sheets (TCSs) using Magnetospheric Multiscale observations from 2017 to 2020
- Plasma thermal pressure alone cannot balance the strong magnetic tension in TCSs
- Off-diagonal pressure components are essential to counteract the strong magnetic tension in TCSs

Supporting Information:

Supporting Information may be found in the online version of this article.

Correspondence to:

S. Lu,
lusan@ustc.edu.cn

Citation:

Zhang, Z., Lu, S., Lu, Q., Wang, R., Li, X., Wang, S., & Artemyev, A. V. (2025). Radial force balance in Earth's magnetotail thin current sheets: MMS observations. *Geophysical Research Letters*, *52*, e2025GL115440. https://doi.org/10.1029/2025GL115440

Received 16 FEB 2025
Accepted 25 JUL 2025

Abstract Thin current sheets (TCS) in Earth's magnetotail are fundamental to magnetospheric dynamics. A key question concerning static magnetotail TCSs is the mechanism of radial force balance. Using the unprecedented measurements from the Magnetospheric Multiscale mission, we statistically analyze TCS crossing events from 2017 to 2020 to investigate this issue. Our analysis reveals a strong magnetic tension within TCSs, with the radial thermal pressure gradient accounts for only 10%–30% of the required balance. The off-diagonal pressure components ($P_{i,xz}$ and $P_{e,xz}$) are crucial for achieving force balance, contributing ∼55% of the required force in the further-Earth region ($-30\ R_E < X < -20\ R_E$, where R_E is Earth's radius), and ∼30% in the near-Earth region ($-20\ R_E < X < -10\ R_E$). This work provides the first direct observational evidence demonstrating that particle kinetic effects (ion nongyrotropy and electron pressure anisotropy) play a significant role in the force balance of magnetotail TCSs.

Plain Language Summary Earth's magnetotail, the region of Earth's magnetic field that is stretched out into space by the solar wind, contains thin layers called thin current sheets (TCSs). These sheets are important for understanding how the magnetotail behaves, especially during space weather events like solar storms. Inside TCSs, strong electrical currents create powerful magnetic forces that pull hot plasma toward Earth. In this study, we used data from NASA's Magnetospheric Multiscale mission to investigate how these TCSs remain in balance under the magnetic tension created by these forces. We found that the pressure from the hot plasma helps counteract the magnetic tension, but only partially—around 10%–30% of the balance. More importantly, we identified additional contributions from a special kind of pressure related to particle motion. These "off-diagonal" pressure components, which arise from complex ion and electron behaviors, account for another 30%–55% of the force needed to maintain balance. Our results provide the first direct spacecraft observations that particle kinetic effects—such as ion nongyrotropy and electron pressure anisotropy—play a key role in keeping TCS stable in Earth's magnetotail. These findings help improve our understanding of space weather and its potential impact on satellites and communications.

1. Introduction

The magnetotail stores magnetic energy converted from the solar wind's energy in the form of a thin current sheet (TCS) with a thickness on the order of ion kinetic scales (Artemyev et al., 2011; S. Lu et al., 2019; Runov et al., 2005; Vasko et al., 2015; Zhang et al., 2024). TCSs are widely recognized as the place where magnetic reconnection occurs (e.g., Genestreti et al., 2023a, 2023b; S. Lu et al., 2020; Q. Lu et al., 2022), which can lead to particle acceleration and global magnetotail reconfiguration during magnetospheric substorms (see review by Sitnov et al. (2019); and references therein). The TCSs have been extensively studied because they are an important element of magnetospheric dynamics. However, our current understanding of the radial force balance within static magnetotail TCSs remains incomplete. The widely accepted model of the magnetotail current sheet describes a two-dimensional magnetic field configuration where hot, dense plasma is concentrated around the neutral plane, and this hot plasma carries cross-tail current density j_y. Note that the Geocentric Solar Magnetospheric (GSM) coordinate system is used here and throughout this paper. Due to the configuration of the magnetic field lines in the magnetotail, the equatorial magnetic field B_z is positive, generating a magnetic tension $j_y B_z$ that acts to push plasma toward Earth (Birn et al., 1977; Kan, 1973; Rich et al., 1972). In isotropic plasma models of

current sheets, this tension is counteracted by the thermal pressure gradient force $\partial P/\partial x$ (e.g., Schindler, 2006), with the equilibrium expressed as $j_y B_z = \partial P/\partial x$. Based on the typical magnetotail parameters (e.g., Huang & Cai, 2009; Rong et al., 2011; Shukhtina et al., 2004), the equilibrium predicts a current density j_y of less than 5 nA/m^2 within the near-Earth's magnetotail.

However, recent observations have revealed that the magnetotail current sheet often maintains a thickness on the order of ion kinetic scales, exhibiting significantly high current densities, typically between 5 and 15 nA/m^2 (e.g., Artemyev et al., 2011; Petrukovich et al., 2015; Runov et al., 2006; Vasko et al., 2015; Zhang et al., 2024), that is, several times larger than the $j_y B_z = \partial P/\partial x$ prediction, which implies that the magnetic tension is too strong to be balanced by the radial (along the tail) gradient of the thermal pressure. It has been posited that balancing this strong magnetic tension requires either pressure anisotropy or nongyrotropy (e.g., see discussion in Sitnov and Merkin (2016) and Artemyev et al. (2021)). In this work, we define "anisotropy" as the condition where the parallel and perpendicular pressures differ ($P_\parallel/P_\perp \neq 1$), while "nongyrotropy" refers to the presence of non-zero off-diagonal components in the pressure tensor even after aligning the coordinate system with the local magnetic field direction. For pressure anisotropy, electrons exhibit $P_{e,\parallel}/P_{e,\perp} > 1$ in magnetotail TCSs, generating $P_{e,xz} = (P_{e,\parallel} - P_{e,\perp})B_x B_z/B^2$ (see Rich et al. (1972)). The electron anisotropy has been found to balance 10%–30% of the magnetic tension (Artemyev et al., 2016). In contrast, ions show negligible anisotropy but are significant demagnetized. The ion demagnetized motion around the equatorial plane is thought to generate off-diagonal pressure components such as $P_{i,xz} \neq 0$, associated with ion nongyrotropy (Ashour-Abdalla et al., 1994; Burkhart et al., 1992; Mingalev et al., 2007). Notably, the electron $P_{e,xz}$ can arise purely from anisotropy in a magnetized plasma, distinct from ion nongyrotropy (which requires demagnetization). Recent particle-in-cell (PIC) simulations by An et al. (2022) and Arnold and Sitnov (2023) have further indicated that the off-diagonal pressure component $P_{xz} \neq 0$ plays a crucial role in the magnetotail CS radial force balance. However, thus far, direct spacecraft observations demonstrating the contribution of off-diagonal pressure component P_{xz} are lacking due to the limitations of plasma measurements in previous missions such as Cluster and THEMIS (see discussion in Artemyev et al. (2019)).

The Magnetospheric Multiscale (MMS, Burch et al., 2016) mission launched by the NASA and providing high-resolution data especially particle pressure tensor. This offers a unique opportunity to investigate the contribution of the off-diagonal pressure component P_{xz} to the pressure balance. In this study, we conduct a statistical analysis of TCS crossing events observed by MMS from 2017 to 2020 to examine the magnitudes of the magnetic tension, the radial thermal pressure gradient force, and the gradient forces of the off-diagonal pressure for these events.

2. Data Set and Methods

To study the radial force balance in TCSs, we utilize magnetic field and plasma data collected by MMS between 2017 and 2020. The magnetic field data are sourced from the Fluxgate Magnetometers with a resolution of 0.1 s (Russell et al., 2016; Torbert et al., 2016), and the plasma data are sourced from the Fast Plasma Investigation (FPI) with resolutions of 4.5 s (Pollock et al., 2017). For TCS crossing events, the four spacecraft of MMS are spaced relatively close together with similar measurements. Therefore, we only use data from MMS1 in this work.

In the previous work (Zhang et al., 2024), we have obtained a data set consisting of 163 thin current sheet crossing events. We have determined the local normal coordinate system for each TCS following the method used in Runov et al. (2006): the **L** direction is directed along the maximum variance eigenvector from Minimum Variance Analysis (MVA, Sonnerup & Scheible, 1998), the **M** direction is along the current density component perpendicular to **L**, and the **N** direction is perpendicular to **L** and **M**. These 163 TCSs have been selected mainly based on the following three criteria. First, the spacecraft must cross or approach the neutral sheet $B_l = 0$. Second, a large current density peak with $j > 5$ nA/m^2 is required to ensure the current sheet is thin enough. Third, the average ion flow speed should be less than 100 km/s to exclude events potentially associated with magnetic reconnection or turbulence. Although the relatively low ion flow speed in our selection criteria could exclude most events associated with magnetic reconnection, it does not exclude electron-only reconnection events. However, the Hall electric field for these events has been estimated in Zhang et al. (2024) to be only a few mV/m (less than 5 mV/m), much smaller than the Hall electric field in reconnection events, which is usually 25 mV/m or greater (e.g., Borg et al., 2005; Eastwood et al., 2010). Therefore, our data set predominantly consists of thin current sheet events in a quiet state. Furthermore, since our study focuses on ion-scale TCSs, any influence from electron-only reconnection is likely negligible in the context of our statistical analysis.

Based on the distribution of the 163 TCS orientations, a fraction of the events exhibits currents that deviate significantly from the nominal dawn-dusk direction. Under the two-fluid approximation and considering particle kinetic effects (such as ion nongyrotropy and electron pressure anisotropy), the detailed force balance equation along the x-direction can be written as:

$$j_y B_z - j_z B_y - \frac{\partial P_{\alpha,xx}}{\partial x} - \frac{\partial P_{\alpha,xy}}{\partial y} - \frac{\partial P_{\alpha,xz}}{\partial z} = 0, \text{with } \alpha = e, i, \tag{1}$$

where j_y and j_z are the current density components, B_y and B_z are the magnetic field components, and $P_{\alpha,xx}$, $P_{\alpha,xy}$, and $P_{\alpha,xz}$ are components of the pressure tensor for ions ($\alpha = i$) and electrons ($\alpha = e$). In this work, we select events that are almost horizontal ($\mathbf{N} \cdot \boldsymbol{e}_z > 0.6$) and in which the currents are predominantly along the dawn-dusk direction ($\mathbf{M} \cdot \boldsymbol{e}_y > 0.6$), resulting in a subset of 104 events. Under these selection criteria, the magnetic tension force in the x-direction is primarily determined by the $j_y B_z$ term, with the contribution from $j_z B_y$ being statistically negligible. Similarly, among the off-diagonal pressure terms, only $P_{\alpha,xz}$ play a significant role in the radial force balance, while $P_{\alpha,xy}$ can be neglected. This simplifies the force balance equation to:

$$j_y B_z - \frac{\partial P_{\alpha,xx}}{\partial x} - \frac{\partial P_{\alpha,xz}}{\partial z} = 0, \text{with } \alpha = e, i. \tag{2}$$

In this work, we use particle moments to calculate the current density $\mathbf{j} = eN_e(\mathbf{V}_i - \mathbf{V}_e)$, where e is the electron charge, N_e is the electron number density, and $\mathbf{V}_i$ ($\mathbf{V}_e$) is the ion (electron) velocity. The TCS thickness for each event is estimated using $L = B_0/(\mu_0 j_0)$, where B_0 is the magnetic field strength at the current sheet boundary and j_0 is the peak value of the current density y-component j_y. The method of determining B_0 is based on single-spacecraft observations of magnetic field, where we assume that the variation of the magnetic field x-component B_x is due to the vertical motion of the TCS with a certain constant velocity. In this case, B_0 is determined as the value at the moment when the rate of B_x variation decreases significantly. This approach may have an error of about 10%–20%, but is relatively reliable for statistical studies (see Artemyev et al. (2010) for details). The magnetic tension for each TCS crossing event is estimated from the average of j_y and B_z in the TCS central region, which is defined as $|B_x| < 0.5B_0$. For our data set, despite the fact that these TCSs are embedded current sheets with narrower current distribution than the plasma distribution, it is still possible to make an approximate description of the currents and thicknesses of single-peak current sheets using magnetic field profile from the Harris model (Artemyev et al., 2011; Harris, 1962; S. Lu et al., 2016). In the central region of a Harris-like current sheet, the magnetic field x-component B_x and the spatial coordinate z vary linearly and the relationship approximately satisfies $B_x/B_0 = z/L$ with an error of less than 10%. Then the force of off-diagonal pressure from the observed P_{xz} and B_x/B_0 can be obtained using the equation:

$$-\frac{\partial P_{xz}}{\partial z} = -\frac{1}{L}\frac{\partial P_{xz}}{\partial (B_x/B_0)}. \tag{3}$$

We use the slopes obtained by fitting the data in the central region as an approximation of $-\partial P_{i,xz}/\partial(B_x/B_0)$ and $-\partial P_{e,xz}/\partial(B_x/B_0)$, which in turn gives us estimates of the forces due to ions and electrons.

3. Results

Figure 1 shows a typical TCS crossing event detected by MMS1 on 12 August 2017, located at (−19.6, −14.4, 2.5) R_E in GSM coordinates. The magnetic field x-component B_x changed from positive to negative from 7.3 to −8.5 nT and reversed at about 01:19:25 UT (Figure 1a), indicating that the spacecraft crossed the neutral sheet from north to south. As shown in Figure 1e, a strong increase of current mainly density along the **y** direction is observed during the spacecraft crossing of the neutral sheet, with a peak current density of $j_0 \approx 9.3$ nA/m^2. All three components of the ion flow velocity were consistently less than 100 km/s in the entire time period (Figure 1c), which suggests that the current sheet was at a quiet time and should be in force equilibrium. The magnitude of the magnetic field at the current sheet boundary, $B_0 \approx 7.9$ nT, is estimated from the extreme values of the B_x component, and the thickness of this current sheet is estimated to be 673 km. The normalized thickness corresponds to approximately 3.8 times the ion inertial length (d_i), which is typical for TCSs (Petrukovich

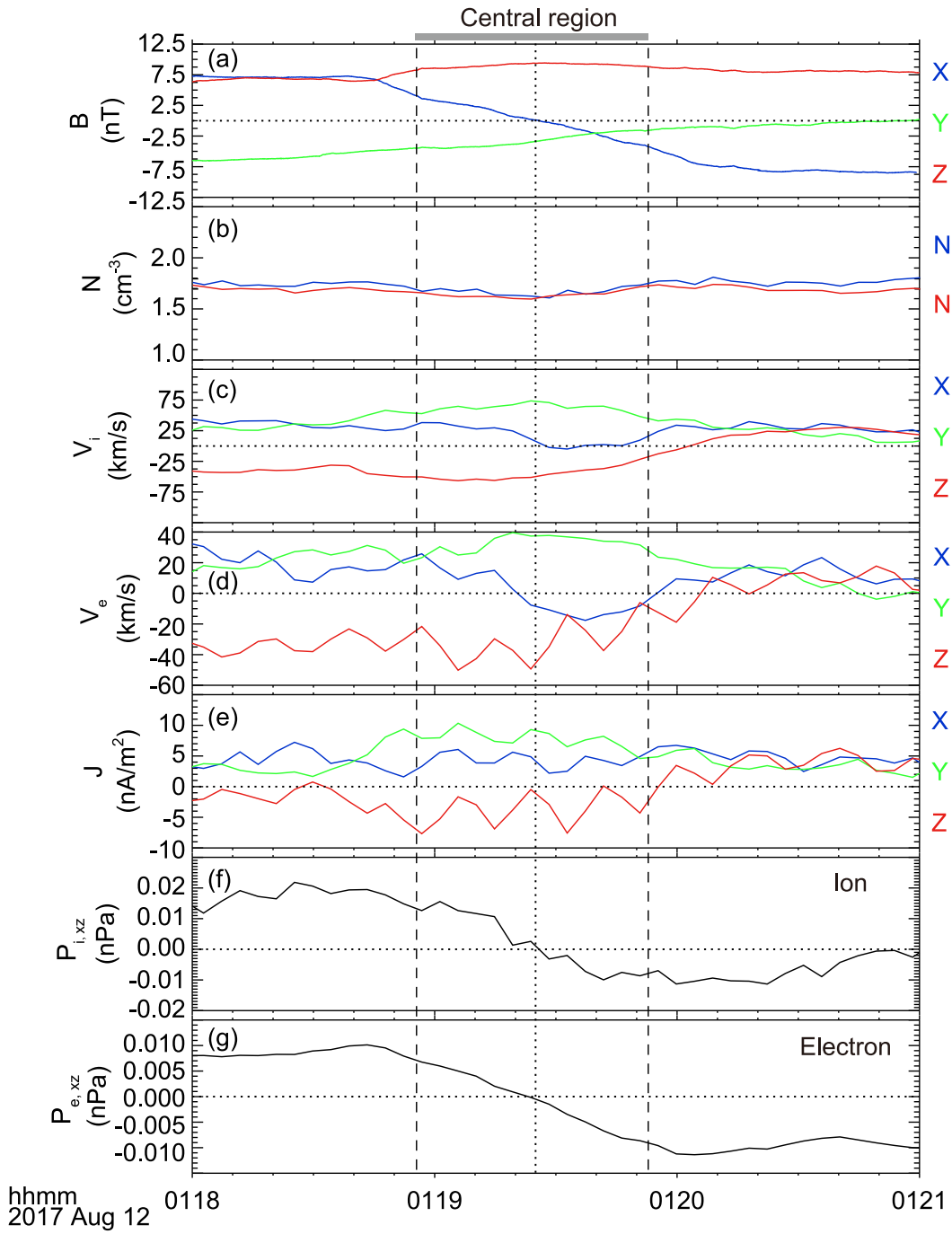

Figure 1. Overview of a typical Thin current sheets (TCS) crossing event observed by MMS1 on 12 August 2017 in Geocentric Solar Magnetospheric coordinates. (a) Magnetic field components. (b) Ion and electron number density. (c) Ion velocity. (d) Electron velocity. (e) Current density in three directions from ion and electron moments. (f, g) Ion and electron pressure tensor non-diagonal term $P_{i,xz}$ and $P_{e,xz}$. The interval between the two vertical dashed lines represents MMS1 crossing the central region of the TCS.

et al., 2015; Zhang et al., 2024). Here, d_i is defined as $d_i = \sqrt{m_i/(\mu_0 N_i e^2)}$, where m_i is the ion mass, μ_0 is the vacuum magnetic permeability, N_i is the ion number density, and e is the elementary charge. Based on the average values of the current density component j_y and the magnetic field component B_z in the TCS central region ($|B_x| < 0.5B_0$), the magnetic tension $j_y B_z$ can be estimated to be about 70.1 nA nT/m^2, pointing toward the Earth.

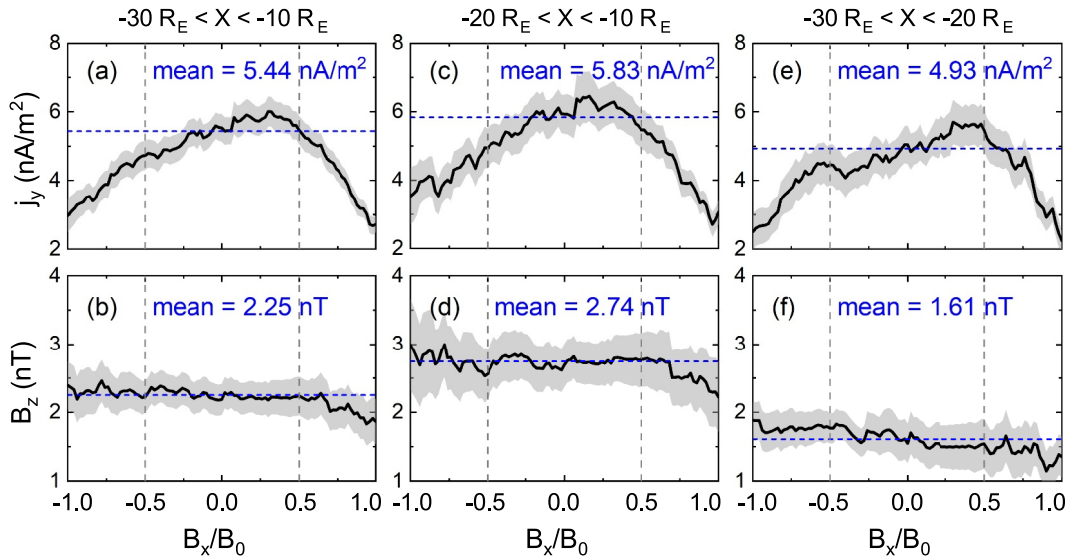

Figure 2. Averaged profiles of the main current density component j_y and the magnetic field component B_z versus B_x/B_0 for Thin current sheets (TCSs) in different regions: (a, b) profiles for all 104 TCSs, (c, d) profiles for the 58 TCSs in the near-Earth region, and (e, f) profiles for the 46 TCSs in the further-Earth region. The bold curves represent the averaged profiles, and the shaded areas indicate the error bands, calculated as the standard error of the mean at each B_x/B_0 bin based on the distributions of individual event values. Vertical dashed lines mark the boundaries of TCS central region and blue horizontal dashed line marks the average values in TCS central region.

Interestingly, as shown in Figures 1f and 1g, the spacecraft observed a clear polarity change from positive to negative in both the ion pressure tensor off-diagonal term $P_{i,xz}$ and the electron pressure tensor off-diagonal term $P_{e,xz}$. With this change in polarity, they can generate gradient forces $-\partial P_{xz}/\partial z$ pointing in the direction away from the Earth to counteract the magnetic tension. Using the TCS thickness and the slopes of $P_{i,xz}$, $P_{e,xz}$ versus B_x/B_0, we obtain the magnitudes of the forces generated by ions and electrons to be 35.3 nA nT/m^2 (50% of j_yB_z) and 24.0 nA nT/m^2 (34% of j_yB_z), respectively. For this current sheet, the gradient forces associated with the demagnetized motion of ions and anisotropic electrons can almost balance the strong magnetic tension, playing an important role in the radial force balance.

Next, we statistically investigate the radial force balance for these 104 TCS events. Figure 2 shows the average profiles of the main current density component j_y and the magnetic field component B_z as functions of B_x/B_0 for TCSs in different regions. Here, the horizontal coordinate B_x/B_0 represents the distance from the neutral sheet, normalized by TCS boundary magnetic field. According to the distance to the Earth, we divide these 104 TCSs into 58 near-Earth events that satisfy $-20\ R_E < X < -10\ R_E$ and 46 further-Earth events that satisfy $-30\ R_E < X < -20\ R_E$. In Figure 2, the bold curves represent the average profiles, and the shaded regions indicate the standard error of the mean at each B_x/B_0 bin. For completeness, the individual event profiles used to construct the averages are provided in Figure S1 in Supporting Information S1. The j_y profiles show a pronounced peak near the neutral sheet, indicating that most of these TCSs are single-peak current sheets with stronger current densities in the central region compared to the edges. On average, B_z is nearly constant and positive at different vertical distances, which is consistent with the configuration of the magnetic lines in the Earth's magnetotail. For all events, the average value of the j_y in the TCS central region is 5.44 nA/m^2 and the average value of the B_z is 2.25 nT, which are in agreement with results obtained by Cluster mission (Artemyev et al., 2016; Petrukovich et al., 2015; Runov et al., 2006). The average magnetic tension j_yB_z of these 104 TCSs can be estimated to be about 12.3 nA nT/m^2. Closer to Earth, j_y increases from 4.93 to 5.83 nA/m^2, and B_z from 1.61 to 2.74 nT, so the magnetic tension also increases, from 9.5 to 14.4 nA nT/m^2. Note that the current density values presented here are the averages within the TCS central region, which are smaller than the peak current density j_0. The j_0 for the 104 TCSs typically ranges from 5 to 15 nA/m^2, which is consistent with previous observations (e.g., Artemyev et al., 2011; Runov et al., 2006). We use the average current density in the central region to estimate magnetic tension, which reflects the overall characteristics of the central region.

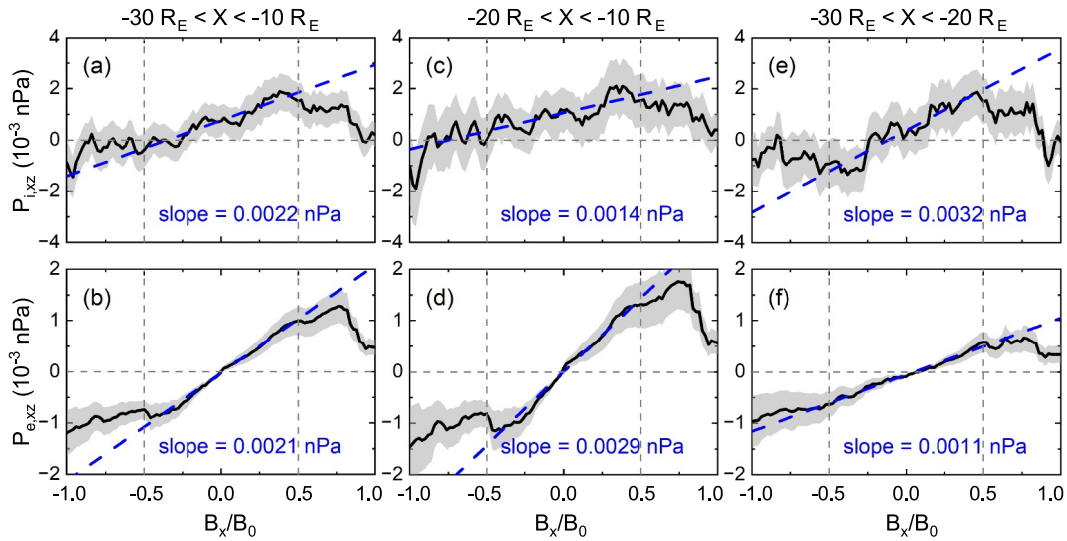

Figure 3. Average profiles of the ion pressure tensor off-diagonal term $P_{i,xz}$ and the electron pressure tensor off-diagonal term $P_{e,xz}$ versus B_x/B_0 for Thin current sheets (TCSs) in different regions. Same format as Figure 2. The blue dashed lines represent the fit to the curves in TCS central region and the blue text show the slopes.

Figure 3 shows the average profiles of the ion pressure tensor off-diagonal term $P_{i,xz}$ and the electron pressure tensor off-diagonal term $P_{e,xz}$ versus B_x/B_0 for TCSs. To facilitate comparison with the magnetic tension results in Figure 2, in addition to the average profiles for all events (Figures 3a and 3b), we also present the profiles separately for near- Earth events (Figures 3c and 3d) and further-Earth events (Figures 3e and 3f). Note that although the events occur during relatively quiet times, P_{xz}, as a second-order moment, is sensitive to uncertainties in the TCS coordinate system (e.g., Rong et al., 2010; Sergeev et al., 2006) and to variations in plasma characteristics. As a result, individual event profiles show large variations. To mitigate these effects, we focus on analyzing the average profiles, and the individual event profiles are provided in Figure S2 in Supporting Information S1 for reference. On average, for both ions and electrons, P_{xz} increases with B_x/B_0, indicating that P_{xz} is stronger in the northern part of the neutral sheet than in the southern part. Consequently, both particles produce a P_{xz} gradient force directed away from the Earth, opposite to the magnetic tension force. Figure 3 also shows that the average P_{xz} in the TCS central region exhibits a nearly linear correlation with the B_x/B_0 and can be approximated with the linear fit, and the slopes of this approximation are shown in blue in the figure. Note a finite P_{xz} at the current sheet center, $B_x = 0$, is likely due to variations (rotations) of TCS local coordinate system, and this small offset can be ignored in evaluation of the pressure gradient. Using $L = B_0/(\mu_0 j_0)$, we estimate that the thickness of these TCSs typically ranges from 500 to 1,500 km, which corresponds to approximately 1–5 times the ion inertial length d_i. The thickness shows no significant variation between near-Earth and further-Earth events, with an overall average of 980 km. The distributions of thickness and current density are provided in Figure S3 in Supporting Information S1. Using these slopes and the average thicknesses of corresponding TCSs, the P_{xz} gradient forces of ions and electrons in different regions can be estimated. For ions, the gradient force $-\partial P_{i,xz}/\partial z$ is about 1.5 nA nT/m^2 in the near-Earth region, corresponds to 10% of the average tension, and it increases to 3.1 nA nT/m^2 in the further-Earth region, accounting for 40% of the tension there. For electrons, the gradient force $-\partial P_{e,xz}/\partial z$ is about 3.1 nA nT/m^2 in the near-Earth region, equivalent to 20% of the average tension, and it is 1.1 nA nT/m^2 in the further-Earth region, representing 15% of the tension. In total, the P_{xz} gradient forces can balance up to 40% of the magnetic tension, playing a significant role in the force equilibrium. This contribution can be even higher for ions due to hot ion component (>25 keV) that is above the FPI energy range (see discussion in Artemyev et al. (2019) and Arnold and Sitnov (2023)).

Finally, we estimate the actual contribution to the force equilibrium generated by the thermal pressure gradient force that is believed to balance the magnetic tension in the traditional 2D CS model. Figure 4 shows the distributions of the pressure tensor diagonal terms P_{xx} ($P_{i,xx}$ and $P_{e,xx}$) with respect to the coordinate X for these 104 TCSs. We use the average values in the TCS central region as $P_{i,xx}$ and $P_{e,xx}$, which represent the thermal pressure near the neutral sheet. As the distance from Earth decreases, $P_{i,xx}$ increases from ∼0.2 to ∼0.4 nPa, while $P_{e,xx}$

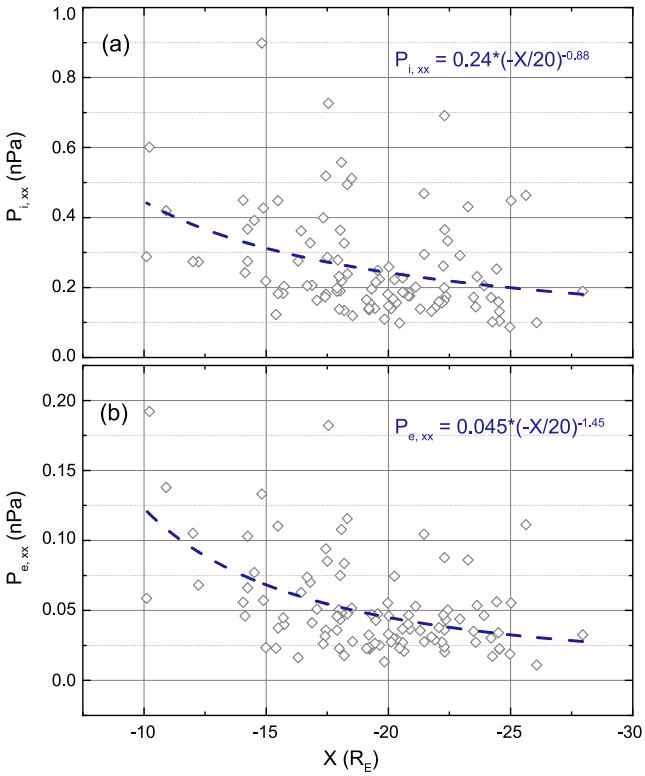

Figure 4. (a) Ion pressure tensor diagonal term $P_{i,xx}$ and (b) electron pressure tensor diagonal term $P_{e,xx}$ for the 104 thin current sheets. Each diamond represents a single event. The blue dashed lines represent exponential fitting results for these data points. The fitting functions are given by: (a) $P_{i,xx} = 0.24\ \text{nPa} \cdot (-X/20\ R_E)^{-0.88}$ and (b) $P_{e,xx} = 0.045\ \text{nPa} \cdot (-X/20\ R_E)^{-1.45}$.

rises from ~0.03 to ~0.12 nPa, indicating an increase in the thermal pressure toward Earth. To estimate the gradient of the thermal pressure, we use an exponential fitting approximation to obtain the relationship between P_{xx} and X, just as it was done in the previous statistical study of the radial distribution of the magnetotail lobe magnetic field (e.g., Artemyev et al., 2016; Zhang et al., 2024). We get the fitting functions for ions and electrons as $P_{i,xx} = 0.24\ \text{nPa} \cdot (-X/20\ R_E)^{-0.88}$ and $P_{e,xx} = 0.045\ \text{nPa} \cdot (-X/20\ R_E)^{-1.45}$, respectively. Using these two functions, the total thermal pressure gradient force $-\partial P_{i,xx}/\partial x - \partial P_{e,xx}/\partial x$ is obtained to be 25% of the magnetic tension for further-Earth events and 15% of the magnetic tension for near- Earth events. The thermal pressure can only contribute 10%–30% of the force balance, which is consistent with previous studies (Artemyev et al., 2016, 2021).

4. Conclusions and Discussion

In this study, we performed a statistical analysis of the radial force equilibrium in 104 magnetotail TCSs using MMS data from 2017 to 2020. For near-Earth events ($-20\ R_E < X < -30\ R_E$), the magnetic tension force was approximately 14.4 nA nT/m^2, with the gradient of the off-diagonal pressure P_{xz} balancing 30% of the tension and the thermal pressure gradient balancing 15%. For further-Earth events ($-10\ R_E < X < -20\ R_E$), the tension force was found to be ~9.5 nA nT/m^2, with the P_{xz} gradient balancing 55% of the tension and the thermal pressure gradient balancing 25%. Overall, we find that there are strong magnetic tension forces exist within TCSs, but the thermal plasma pressure only accounts for around 20% of the required balance. The off-diagonal pressure P_{xz} is significant for maintaining radial equilibrium, balancing between 30% and 55% of the strong magnetic tension.

Our statistical analysis reveals that both ion and electron off-diagonal pressures ($P_{i,xz}$ and $P_{e,xz}$) contribute significantly to the radial force balance in TCSs. In TCSs with ion-scale thickness, ions are mostly demagnetized and move along quasi-adiabatic orbits, resulting in significant $P_{i,xz} \neq 0$, indicative of ion nongyrotropy. For electrons, although they are mostly magnetized, we still observe a nonzero $P_{e,xz}$, which can be attributed to the electron pressure anisotropy ($P_{e\parallel}/P_{e\perp} > 1$, Artemyev et al., 2016; Zhang et al., 2024). Such a nonzero $P_{e,xz}$ helps balance 15%–20% of the magnetic tension, consistent with THEMIS observations by Artemyev et al. (2016). Although these off-diagonal pressures support a quasi-equilibrium force balance, they also make the system highly sensitive to small perturbations. As suggested by An et al. (2022), small deviations in these delicate contributions can locally enhance the current density and promote destabilization. In particular, Ion nongyrotropy $P_{i,xz} \neq 0$ can promote Landau resonance and ion tearing instabilities, while electron pressure anisotropy $P_{e\parallel}/P_{e\perp} > 1$ can generate electron-scale instabilities (Karimabadi et al., 2004; S. Lu et al., 2020; Pritchett, 2005, and references therein). Therefore, despite contributing to equilibrium, these kinetic effects also render TCS more prone to reconnection onset.

While the significant contributions of off-diagonal pressures are revealed, we acknowledge that the balance is not fully achieved. Our statistical analysis indicates that for near-Earth events, approximately 55% of the magnetic tension remains unbalanced, while for further-Earth events, about 20% remains unbalanced. Several factors may account for this incomplete balance, including uncertainties in P_{xz} measurements (primarily due to missing high energy ion population and possible contribution of heavy oxygen ions), the dynamic nature of the magnetotail, the contribution from the turbulence, and potential underestimation of the thermal pressure gradient. Future studies are needed to more accurately quantify and account for these effects. Furthermore, we note that retaining only the 60% thinner current sheet events ($L < 3d_i$) shows a larger relative contribution from P_{xz} (see Figure S4 in Supporting Information S1). This suggests that current sheet thickness may influence the P_{xz} contribution and thus warrants further investigation. This study provides the first observational evidence demonstrating the significant contribution of particle kinetic effects to the magnetotail TCS force balance, thus underscoring the vital importance of incorporating this effect accurately into future magnetotail models.

Data Availability Statement

All the MMS data used in this study can be downloaded at the MMS data center (https://lasp.colorado.edu/mms/sdc/). We used the software SPEDAS V4.1 (Version 4.1) (Angelopoulos et al., 2019) for data access and processing, which is available at the page https://spedas.org/.

Acknowledgments
This work was supported by the NSFC Grants 42274196 and 42230201, and the Strategic Priority Research Program of the Chinese Academy of Sciences (Grants XDB0560000 and XDB41000000). We sincerely thank the entire MMS team and instrument principal investigators for their contributions in providing and calibrating the data.

References

An, X., Artemyev, A. V., Angelopoulos, V., Runov, A., Lu, S., & Pritchett, P. (2022). Configuration of magnetotail current sheet prior to magnetic reconnection onset. *Geophysical Research Letters*, *49*(6), e2022GL097870. https://doi.org/10.1029/2022GL097870

Angelopoulos, V., Cruce, P., Drozdov, A., Grimes, E. W., Hatzigeorgiu, N., King, D. A., et al. (2019). The space physics environment data analysis system (version 4.1) [Software]. *Space Science Reviews*, *215*(1), 9. https://doi.org/10.1007/s11214-018-0576-4

Arnold, H., & Sitnov, M. I. (2023). PIC simulations of overstretched ion-scale current sheets in the magnetotail. *Geophysical Research Letters*, *50*(15), e2023GL104534. https://doi.org/10.1029/2023GL104534

Artemyev, A. V., Lu, S., El-Alaoui, M., Lin, Y., Angelopoulos, V., Zhang, X.-J., et al. (2021). Configuration of the Earth's magnetotail current sheet. *Geophysical Research Letters*, *48*(6), e2020GL092153. https://doi.org/10.1029/2020GL092153

Artemyev, A. V., Angelopoulos, V., & Runov, A. (2016). On the radial force balance in the quiet time magnetotail current sheet. *Journal of Geophysical Research: Space Physics*, *121*(5), 4017–4026. https://doi.org/10.1002/2016JA022480

Artemyev, A. V., Angelopoulos, V., Vasko, I. Y., Zhang, X.-J., Runov, A., & Zelenyi, L. M. (2019). Ion anisotropy in Earth's magnetotail current sheet: Multicomponent ion population. *Journal of Geophysical Research: Space Physics*, *124*(5), 3454–3467. https://doi.org/10.1029/2019JA026604

Artemyev, A. V., Petrukovich, A. A., Nakamura, R., & Zelenyi, L. M. (2010). Proton velocity distribution in thin current sheets: Cluster observations and theory of transient trajectories. *Journal of Geophysical Research*, *115*(A12), A12255. https://doi.org/10.1029/2010JA015702

Artemyev, A. V., Petrukovich, A. A., Nakamura, R., & Zelenyi, L. M. (2011). Cluster statistics of thin current sheets in the Earth magnetotail: Specifics of the dawn flank, proton temperature profiles and electrostatic effects. *Journal of Geophysical Research*, *116*(A9), A09233. https://doi.org/10.1029/2011JA016801

Ashour-Abdalla, M., Zelenyi, L. M., Peroomian, V., & Richard, R. L. (1994). Consequences of magnetotail ion dynamics. *Journal of Geophysical Research*, *99*(A8), 14891–14916. https://doi.org/10.1029/94JA00141

Birn, J., Sommer, R. R., & Schindler, K. (1977). Self-consistent theory of the quiet magnetotail in three dimensions. *Journal of Geophysical Research*, *82*(1), 147–154. https://doi.org/10.1029/JA082i001p00147

Borg, A. L., Øieroset, M., Phan, T. D., Mozer, F. S., Pedersen, A., Mouikis, C., et al. (2005). Cluster encounter of a magnetic reconnection diffusion region in the near-Earth magnetotail on September 19, 2003. *Geophysical Research Letters*, *32*(19), L19105. https://doi.org/10.1029/2005GL023794

Burch, J. L., Moore, T. E., Torbert, R. B., & Giles, B. L. (2016). Magnetospheric multiscale overview and science objectives. *Space Science Reviews*, *199*(1), 5–21. https://doi.org/10.1007/s11214-015-0164-9

Burkhart, G. R., Drake, J. F., Dusenbery, P. B., & Speiser, T. W. (1992). A particle model for magnetotail neutral sheet equilibria. *Journal of Geophysical Research*, *97*(A9), 13799–13815. https://doi.org/10.1029/92JA00495

Eastwood, J. P., Phan, T. D., Øieroset, M., & Shay, M. A. (2010). Average properties of the magnetic reconnection ion diffusion region in the Earth's magnetotail: The 2001–2005 cluster observations and comparison with simulations. *Journal of Geophysical Research*, *115*(A8), 2009JA014962. https://doi.org/10.1029/2009JA014962

Genestreti, K. J., Farrugia, C. J., Lu, S., Vines, S. K., Reiff, P. H., Phan, T., et al. (2023a). Multiscale observation of magnetotail reconnection onset: 1. Macroscopic dynamics. *Journal of Geophysical Research: Space Physics*, *128*(11), e2023JA031758. https://doi.org/10.1029/2023JA031758

Genestreti, K. J., Farrugia, C. J., Lu, S., Vines, S. K., Reiff, P. H., Phan, T., et al. (2023b). Multi-scale observation of magnetotail reconnection onset: 2. Microscopic dynamics. *Journal of Geophysical Research: Space Physics*, *128*(11), e2023JA031760. https://doi.org/10.1029/2023JA031760

Harris, E. G. (1962). On a plasma sheath separating regions of oppositely directed magnetic field. *Il Nuovo Cimento - B*, *23*(1), 115–121. https://doi.org/10.1007/BF02733547

Huang, C.-S., & Cai, X. (2009). Magnetotail total pressure and lobe magnetic field at onsets of sawtooth events and their relation to the solar wind. *Journal of Geophysical Research*, *114*(A4), A04204. https://doi.org/10.1029/2008JA013807

Kan, J. R. (1973). On the structure of the magnetotail current sheet. *Journal of Geophysical Research*, *78*(19), 3773–3781. https://doi.org/10.1029/JA078i019p03773

Karimabadi, H., Daughton, W., & Quest, K. B. (2004). Role of electron temperature anisotropy in the onset of magnetic reconnection. *Geophysical Research Letters*, *31*(18), L18801. https://doi.org/10.1029/2004GL020791

Lu, Q., Fu, H., Wang, R., & Lu, S. (2022). Collisionless magnetic reconnection in the magnetosphere. *Chinese Physics B*, *31*(8), 089401. https://doi.org/10.1088/1674-1056/ac76ab

Lu, S., Artemyev, A. V., Angelopoulos, V., Lin, Y., Zhang, X.-J., Liu, J., et al. (2019). The hall electric field in Earth's magnetotail thin current sheet. *Journal of Geophysical Research: Space Physics*, *124*(2), 1052–1062. https://doi.org/10.1029/2018JA026202

Lu, S., Lin, Y., Angelopoulos, V., Artemyev, A. V., Pritchett, P. L., Lu, Q., & Wang, X. Y. (2016). Hall effect control of magnetotail dawn-dusk asymmetry: A three-dimensional global hybrid simulation. *Journal of Geophysical Research: Space Physics*, *121*(12), 11882–11895. https://doi.org/10.1002/2016JA023325

Lu, S., Wang, R., Lu, Q., Angelopoulos, V., Nakamura, R., Artemyev, A. V., et al. (2020). Magnetotail reconnection onset caused by electron kinetics with a strong external driver. *Nature Communications*, *11*(1), 5049. https://doi.org/10.1038/s41467-020-18787-w

Mingalev, O. V., Mingalev, I. V., Malova, K. V., & Zelenyi, L. M. (2007). Numerical simulations of plasma equilibrium in a one-dimensional current sheet with a nonzero normal magnetic field component. *Plasma Physics Reports*, *33*(11), 942–955. https://doi.org/10.1134/S1063780X07110062

Petrukovich, A., Artemyev, A. V., Vasko, I., Nakamura, R., & Zelenyi, L. (2015). Current sheets in the Earth magnetotail: Plasma and magnetic field structure with cluster project observations. *Space Science Reviews*, *188*(1), 311–337. https://doi.org/10.1007/s11214-014-0126-7

Pollock, C., Moore, T., Jacques, A., Burch, J., Gliese, U., Saito, Y., et al. (2017). Fast plasma investigation for magnetospheric multiscale. *Magnetospheric Multiscale*, *199*(1), 329–404. https://doi.org/10.1007/978-94-024-0861-4_12

Pritchett, P. L. (2005). Externally driven magnetic reconnection in the presence of a normal magnetic field. *Journal of Geophysical Research*, *110*(A5), A05209. https://doi.org/10.1029/2004JA010948

Rich, F. J., Vasyliunas, V. M., & Wolf, R. A. (1972). On the balance of stresses in the plasma sheet. *Journal of Geophysical Research*, *77*(25), 4670–4676. https://doi.org/10.1029/JA077i025p04670

Rong, Z. J., Shen, C., Petrukovich, A. A., Wan, W. X., & Liu, Z. X. (2010). The analytic properties of the flapping current sheets in the earth magnetotail. *Planetary and Space Science*, *58*(10), 1215–1229. https://doi.org/10.1016/j.pss.2010.04.016

Rong, Z. J., Wan, W. X., Shen, C., Li, X., Dunlop, M. W., Petrukovich, A. A., et al. (2011). Statistical survey on the magnetic structure in magnetotail current sheets. *Journal of Geophysical Research*, *116*(A9), A09218. https://doi.org/10.1029/2011JA016489

Runov, A., Sergeev, V. A., Baumjohann, W., Nakamura, R., Apatenkov, S., Asano, Y., et al. (2005). Electric current and magnetic field geometry in flapping magnetotail current sheets. *Annales Geophysicae*, *23*(4), 1391–1403. https://doi.org/10.5194/angeo-23-1391-2005

Runov, A., Sergeev, V. A., Nakamura, R., Baumjohann, W., Apatenkov, S., Asano, Y., et al. (2006). Local structure of the magnetotail current sheet: 2001 cluster observations. *Annales Geophysicae*, *24*(1), 247–262. https://doi.org/10.5194/angeo-24-247-2006

Russell, C. T., Anderson, B. J., Baumjohann, W., Bromund, K. R., Dearborn, D., Fischer, D., et al. (2016). The magnetospheric multiscale magnetometers. *Space Science Reviews*, *199*(1), 189–256. https://doi.org/10.1007/s11214-014-0057-3

Schindler, K. (2006). *Physics of space plasma activity*. Cambridge University Press.

Sergeev, V. A., Sormakov, D. A., Apatenkov, S. V., Baumjohann, W., Nakamura, R., Runov, A. V., et al. (2006). Survey of large-amplitude flapping motions in the midtail current sheet. *Annales Geophysicae*, *24*(7), 2015–2024. https://doi.org/10.5194/angeo-24-2015-2006

Shukhtina, M. A., Dmitrieva, N. P., & Sergeev, V. A. (2004). Quantitative magnetotail characteristics of different magnetospheric states. *Annales Geophysicae*, *22*(3), 1019–1032. https://doi.org/10.5194/angeo-22-1019-2004

Sitnov, M. I., Birn, J., Ferdousi, B., Gordeev, E., Khotyaintsev, Y., Merkin, V., et al. (2019). Explosive magnetotail activity. *Space Science Reviews*, *215*(4), 31. https://doi.org/10.1007/s11214-019-0599-5

Sitnov, M. I., & Merkin, V. G. (2016). Generalized magnetotail equilibria: Effects of the dipole field, thin current sheets, and magnetic flux accumulation. *Journal of Geophysical Research: Space Physics*, *121*(8), 7664–7683. https://doi.org/10.1002/2016JA023001

Sonnerup, B. U. O., & Scheible, M. P. (1998). Minimum and maximum variance analysis. Retrieved from https://api.semanticscholar.org/CorpusID:118577335

Torbert, R. B., Russell, C. T., Magnes, W., Ergun, R. E., Lindqvist, P.-A., LeContel, O., et al. (2016). The FIELDS instrument suite on MMS: Scientific objectives, measurements, and data products. *Space Science Reviews*, *199*(1), 105–135. https://doi.org/10.1007/s11214-014-0109-8

Vasko, I. Y., Petrukovich, A. A., Artemyev, A. V., Nakamura, R., & Zelenyi, L. M. (2015). Earth's distant magnetotail current sheet near and beyond lunar orbit. *Journal of Geophysical Research: Space Physics*, *120*(10), 8663–8680. https://doi.org/10.1002/2015JA021633

Zhang, Z., Lu, S., Lu, Q., Wang, R., Zhan, C., Li, X., & Artemyev, A. V. (2024). Statistical survey of thin current sheets in Earth's magnetotail: MMS observations. *Journal of Geophysical Research: Space Physics*, *129*(5), e2024JA032575. https://doi.org/10.1029/2024JA032575